Central Electron Temperature Measurement by Third-Harmonic Electron-Cyclotron Emission from the Heliotron-*E* Currentless Plasma

J. N. Talmadge,[a] H. Zushi, S. Sudo, T. Mutoh, M. Sato, T. Obiki, O. Motojima, A. Iiyoshi, and K. Uo
Plasma Physics Laboratory, Kyoto University, Gokasho, Uji, Japan

(Received 23 May 1983)

The dependence of the optically thin third-harmonic emission on the electron density and temperature was observed to be in good agreement with theory. A one-dimensional model is used to show that the effect on calculating the central electron temperature of density profile variations is minimal, while that of temperature profile changes is small if the variations are within reasonable limits. Comparison of the temperature evolution calculated by use of the third-harmonic emission with shot-to-shot Thomson scattering shows very good agreement.

PACS numbers: 52.55.Gb, 52.70.Gw

The electron-cyclotron emission from a plasma has usually been observed at the first or second harmonics where the plasma radiates like a blackbody.[1] However, if the local plasma density is greater than the cutoff density, then there exist evanescent regions in the plasma through which the radiation cannot propagate to the detection system. In this case, the third-harmonic emission can theoretically be used to obtain the local electron temperature and density, even though the emission is generally not blackbody.[2] In tokamaks, where previous third-harmonic measurements have been made,[3-5] the toroidal electric field necessary to drive an Ohmic current may give rise to a small population of runaway electrons. The nonthermal emission from these electrons often masks the thermal emission at the higher harmonics even though the emission at the lower harmonics may be relatively unaffected by these energetic electrons.[6] We have produced a plasma in the Heliotron-*E* device without using a toroidal electric field and have studied the third-harmonic emission from the thermal plasma. In this Letter, we present the first verification of the dependence of the third-harmonic optically thin emission on the electron temperature and density using an optical depth that is valid when $\omega_{pe}/\omega_{ce} \geq 1$.

The specific intensity for optically thin ($\tau \ll 1$) emission is given by the following relation[7]:

$$I = \frac{I_b(1-e^{-\tau})}{1-\rho e^{-\tau}} \simeq \frac{I_b \tau(n_e, T_e)}{1-\rho}, \tag{1}$$

where I_b is the vacuum blackbody intensity ($I_b = \omega^2 k T_e/8\pi^3 c^2$), τ is the optical depth, ρ is the power reflectivity of the vacuum vessel walls, and it is assumed here that $1-\rho \gg \rho\tau$. Previous papers on third-harmonic cyclotron emission used the low-density optical-depth approximation ($\omega_{pe} \ll \omega_{ce}$) for the extraordinary mode derived by Engelmann and Curatolo.[2] For typical Heliotron-*E* parameters $\omega_{pe} \geq \omega_{ce}$, so that it is necessary to use the more accurate equation derived by Bornatici,[8]

$$\tau_3 = \frac{81\pi}{4}\frac{\omega_{pe}^2}{\omega_{ce}^2}\left(\frac{72-18\omega_{pe}^2/\omega_{ce}^2+\omega_{pe}^4/\omega_{ce}^4}{72-9\omega_{pe}^2/\omega_{ce}^2}\right)^{3/2}\left(\frac{24-2\omega_{pe}^2/\omega_{ce}^2}{24-3\omega_{pe}^2/\omega_{ce}^2}\right)^2\left(\frac{kT_e}{2mc^2}\right)^2\frac{B}{dB/ds}, \tag{2}$$

where ω_{pe} is the plasma frequency, ω_{ce} is the cyclotron frequency, B is the magnetic field, and dB/ds is the gradient of the magnetic field along the path of the emission. Typically the optical depth for third-harmonic emission in Heliotron-*E* is less than 0.03. With use of the method of Laurent and Brossier,[5] indications are that the wall reflectivity is on the order of 0.92, justifying the neglection of the $\rho\tau$ term in Eq. (1). Combining Eqs. (1) and (2), the specific intensity from a particular position in the plasma can be written as $I \propto Z(n_e) T_e^3$.

To model the total emission observed by the radiometer we use a one-dimensional approximation,

$$I_{\text{tot}} = \int_0^1 I(x)\,dx \propto \int_0^1 Z(n_e(x))\, T_e(x)^3\,dx,$$
$$n_e(x) = n_0(1-x^p), \quad T_e(x) = T_{e0}(1-x^q), \tag{3}$$

where $x \equiv r/a$, and a is the minor plasma radius. The integration is performed over a $|B| = \text{const}$ line in the plasma. To test the effect of variations in the density and temperature profiles on calculating the central electron temperature T_{e0}, we plot the ratio of the total emission received by

the horn to the emission from the plasma center, $K = I_{tot}/Z(n_0)T_{e0}^3$, as a function of average density for various profiles. Sample profiles given by p or q are shown in Fig. 1(a).

Experimentally, it is not always possible to know the density in the plasma core very accurately. Rather, what is usually available is the line-averaged density provided by a microwave interferometer. Thus in computing the quantity $Z(n_0)$ we use $n_0 = 1.5\bar{n}$ (where $\bar{n}$ is the average density), corresponding to $p = 2.0$ (parabolic density profile) regardless of the actual profile. Figure 1(b) shows that K is relatively constant as a function of density and profile factor p and blows up at average densities greater than 3.5×10^{13} cm^{-3} as the emission from the plasma core is cut off. As long as the profile is between $p = 1.0$ and $p = 8.0$, the error in the calculated temperature below an average density of 2.5×10^{13} cm^{-3} will be on the order of 5% or less. The effect of changes in the temperature profile is more important as shown in Fig. 1(c). As q is increased to 8.0 (flat profile), K increases by 1.6 leading to an overestimation of the temperature by +17%. Similarly, as q is decreased from 2.0 to 1.0 (peaked profile) there will be an error in calculating the temperature of −17%.

The model, as developed above, is an estimate of the maximum extent that profile effects may be important because it accords equal weight to the radiation observed directly and the radiation detected because of wall reflections. It does not take into account the depolarization of the radiation due to reflections. However, as shown by Hutchinson and Komm,[9] because the optical depth for the ordinary mode is down by a factor of $(v_{thermal}/c)^2$ from the extraordinary mode, the observed emission is still proportional to $I_b \tau_{ext}$ when the depolarization effect is included. Also, by using the optical depth valid for quasiperpendicular propagation we have neglected the possibility that wall reflections will redirect radiation emitted in the Doppler regime into the radiometer. We estimate, using a model similar to Clark's,[3] that the error in determining the central electron temperature while neglecting this effect will only be on the order of 1%.

This model can now be related to the experimental observation of the third-harmonic emission from a currentless plasma in Heliotron-E.[10] A hydrogen plasma is produced and heated by electron-cyclotron resonance heating by means of a 28-GHz gyrotron with a pulse width of 10 msec and rf power of 70 kW.[11] About 6 msec after the rf has been turned on, about 1 MW of neutral beams is injected into the plasma for a duration of 50–60 msec. The diagnostic used to observe the third-harmonic emission consists of a standard heterodyne receiver with a sweepable backward-wave oscillator. In the present experiment, with the magnetic field at 1.0 T, the frequency was fixed at 85 GHz ($\simeq 3f_{ce0}$). The receiver bandwidth Δf was 500 MHz which determined the radial resolution to be about 3 cm in the center of the plasma. The acceptance angle of the antenna was ± 4° which, with neglect of refraction effects, determined the vertical resolution to be 8 cm. The extraordinary-mode emission was received by a horn which was located in a direction outward along a major radius, outside the vacuum tank. As seen in Fig. 4, the radiated power at the third harmonic was very high at the beginning of the rf pulse, characteristic of nonthermal emission emitted during the initial

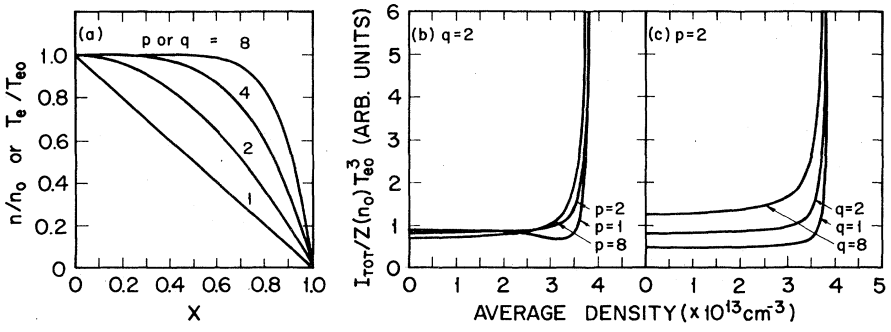

FIG. 1. (a) Profiles given by $Y = Y_0(1 - x^z)$, where Y is the electron density or temperature and z is p or q, respectively. Also shown is the ratio of the total emission received by the radiometer I_{tot} to the emission from the center $Z(n_0)T_{e0}^3$ ($n_0 = 1.4\bar{n}$, where $\bar{n}$ is the average density) vs the line-averaged density for various (b) density and (c) temperature profiles.

breakdown of the gas. As the density increased from 0.6 to 3.0×10^{13} cm^{-3} during the neutral-beam–injection phase, this nonthermal component decreased very rapidly. It is important to note that at a peak density of 2×10^{13} cm^{-3} (average density of 1.3×10^{13} cm^{-3}) the second-harmonic emission was cut off and only the third harmonic could be detected.

We tested the experimental validity of the relation $I/Z(n_0)\propto T_e^3$ in the following manner: The intensity of the third-harmonic emission was measured during the course of two consecutive days, at which time the density varied from 0.6×10^{13} to 3.5×10^{13} cm^{-3} and the temperature varied from 200 to 600 eV. Simultaneously, a 2-mm microwave interferometer monitored the time evolution of the line-averaged electron density. Also, a multichannel laser–Thomson-scattering system measured the temperature profile at a single instant of time every discharge. The ratio $I/Z(n_0)$ was then calculated, where I is the output of the radiometer in millivolts and $Z(n_0)$ is computed from the interferometer under the assumption that $n_0=1.5\,\bar{n}$. This ratio was then compared to the larger temperature of the two central channels of the Thomson-scattering system that fell within the resolution of the radiometer. The result of the experiment is shown in Fig. 2. Omitted from the figure are data points that correspond to a time early in the discharge when the cyclotron emission was nonthermal and those points where the error bar in the Thomson-scattering data was greater than 15%. The solid curve is the best cubic fit to the data points and shows good agreement between the experimental data and theory. Approximately $\frac{2}{3}$ of the data points lie within the Thomson-scattering error bar from the curve that represents the best cubic fit.

It is interesting to investigate in further detail two of the points on the graph that do not lie within the Thomson-scattering error bar, labeled (a) and (b) on the graph. If we compare the temperature measured by the radiometer to the Thomson-scattering measurement, point (a), which lies to the right of the solid line, has an error of about -20%. Point (b), on the other hand, lies to the left of the solid line and has an error of about $+19\%$. Figure 3 shows the temperature profiles for the two data points, based on the Thomson-scattering data. Profile (a) can be fitted by a curve given by $T_e=400(1-x)$ while profile (b) can be fitted by a curve given by $T_e=415(1-x^8)$. From Fig. 1, the error calculated theoretically was -17% for point (a) and $+17\%$ for point (b). Considering the error in the Thomson-scattering temperature and the relative simplicity of the theoretical model, this shows good

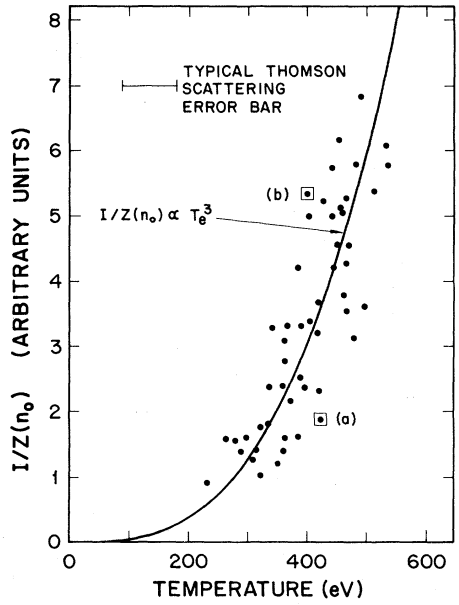

FIG. 2. Ratio of the emission received by the radiometer I to the function $Z(n_0)$ ($n_0=1.5\bar{n}$, and $\bar{n}$ is the density measured by a microwave interferometer) vs the electron temperature measured by laser Thomson scattering. The curve is the best cubic fit to the data.

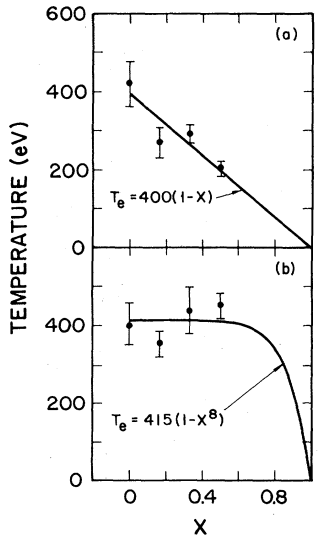

FIG. 3. Electron temperature profile measured by Thomson scattering for two points labeled (a) and (b) in Fig. 2.

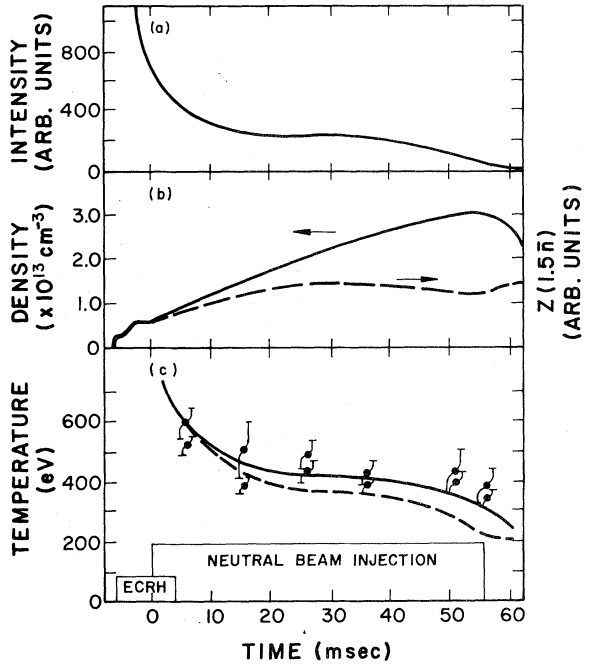

FIG. 4. (a) Third-harmonic cyclotron emission. (b) Density measured by a microwave interferometer (solid line) and the calculated function $Z(1.5\bar{n})$ as given in the text (broken line). (c) Time evolution of the electron temperature as computed from (a) and (b) above and the best cubic fit from Fig. 2 (solid line). Also shown are the shot-to-shot Thomson-scattering temperatures and the temperature calculated with the low-density optical-depth approximation (broken line).

agreement between theory and experiment. Thus, it can be concluded that the optically thin third harmonic can accurately determine the electron temperature as long as the temperature profile does not vary over too broad a range.

It is now possible to compare the time evolution of the electron temperature during electron-cyclotron resonance heating and neutral beam injection from the third-harmonic emission and the line-averaged density with the shot-to-shot Thomson-scattering data. Shown in Fig. 4 are the third-harmonic emission, the interferometer signal, the function $Z(1.5\bar{n})$, and the computed electron temperature from the best cubic fit of Fig. 2. The greater of the two temperatures measured by the central channels of the Thomson-scattering system are shown in the figure and were obtained under a fixed set of plasma conditions. It can be seen that the agreement between the radiometer and the Thomson-scattering data is very good. Also shown in the figure is the electron temperature calculated with use of the low-density optical-depth approximation ($\tau_{ext} \propto n$). It should be noted that significant errors result at the higher densities when this approximation is used.

In summary, it has been shown that the cyclotron emission at the third harmonic can be used to accurately determine the central electron temperature. This technique becomes especially useful when the density is so great that the blackbody second-harmonic emission is cut off.

The authors would like to thank Dr. K. Kondo, Dr. H. Kaneko, Dr. S. Besshou, Dr. F. Sano, Dr. A. Sasaki, and Dr. T. Mizuuchi for their support. This work was supported in part by the U. S. Department of Energy under Contract No. DE-AC02-78ET53082. One of us (J.N.T.) would also like to thank the staff at the Heliotron Center for allowing him the opportunity to work with them.

[a]Permanent address: Torsatron-Stellarator Laboratory, University of Wisconsin, Madison, Wisc. 53706.

[1]P. C. Efthimion, V. Arunasalam, R. A. Bitzer, and J. C. Hosea, *Temperature* (Reinhold, New York, 1982), Vol. 5.

[2]F. Engelmann and M. Curatolo, Nucl. Fusion 13, 497 (1973).

[3]W. H. M. Clark, Culham Laboratory Report No. CLM-P 673, 1983 (unpublished).

[4]F. J. Stauffer and D. A. Boyd, Infrared Phys. 18, 755 (1978).

[5]L. Laurent and Ph. Brossier, Association Euratom–Commissariat á l'Energie Atomique Report No. EUR-CEA-FC-1112, 1981 (unpublished).

[6]C. M. Celata and D. A. Boyd, Nucl. Fusion 17, 735 (1977).

[7]G. Bekefi, *Radiation Processes in Plasmas* (Wiley, New York, 1966).

[8]M. Bornatici, Plasma Phys. 24, 629 (1982).

[9]I. H. Hutchinson and D. S. Komm, Nucl. Fusion 17, 1077 (1977).

[10]K. Uo *et al.*, in *Proceedings of the Eigth International Conference on Plasma Physics and Controlled Nuclear Fusion Research, Brussels, 1980* (International Atomic Energy Agency, Vienna, 1981), Vol. 1, p. 217.

[11]A. Iiyoshi *et al.*, Phys. Rev. Lett. 48, 745 (1982).